JOURNAL OF GEOPHYSICAL RESEARCH, VOL. 102, NO. E12, PAGES 28,717–28,723, DECEMBER 25, 1997

Rate coefficients for reactions of ethynyl radical (C_2H) with HCN and CH_3CN: Implications for the formation of complex nitriles on Titan

Ray J. Hoobler and Stephen R. Leone

JILA, National Institute of Standards and Technology and University of Colorado, Boulder
Department of Chemistry and Biochemistry, University of Colorado, Boulder

Abstract. Rate coefficients for the reactions of C_2H + HCN → products and C_2H + CH_3CN → products have been measured over the temperature range 262–360 K. These experiments represent an ongoing effort to accurately measure reaction rate coefficients of the ethynyl radical, C_2H, relevant to planetary atmospheres such as those of Jupiter and Saturn and its satellite Titan. Laser photolysis of C_2H_2 is used to produce C_2H, and transient infrared laser absorption is employed to measure the decay of C_2H to obtain the subsequent reaction rates in a transverse flow cell. Rate constants for the reaction C_2H + HCN → products are found to increase significantly with increasing temperature and are measured to be (3.9–6.2) × 10^{-13} cm^3 $molecules^{-1}$ s^{-1} over the temperature range of 297–360 K. The rate constants for the reaction C_2H + CH_3CN → products are also found to increase substantially with increasing temperature and are measured to be (1.0–2.1) × 10^{-12} cm^3 $molecules^{-1}$ s^{-1} over the temperature range of 262–360 K. For the reaction C_2H + HCN → products, ab initio calculations of transition state structures are used to infer that the major products form via an addition/elimination pathway. The measured rate constants for the reaction of C_2H + HCN → products are significantly smaller than values currently employed in photochemical models of Titan, which will affect the HC_3N distribution.

1. Introduction

Over the last 2 years there have been two new photochemical models of Titan's atmosphere [*Lara et al.*, 1996; *Toublanc et al.*, 1995]. These models differ from the first post-Voyager model [*Yung et al.*, 1984; *Yung*, 1987] primarily in the updated methane photodissociation scheme [*Mordaunt et al.*, 1993], better characterizations of the eddy diffusion coefficient, and updated reaction rates. *Gladstone et al.* [1996] also presented a photochemical model for the upper atmosphere of Jupiter based on similar reaction sequences.

With the upcoming Cassini/Huygens mission to Saturn and its largest satellite Titan, there is renewed interest in understanding the photochemical processes that take place in the atmosphere of Titan. This interest generally arises from the presence of a dense N_2-CH_4 atmosphere which is thought to possess many similarities with the prebiotic chemistry of the Earth [*Raulin et al.*, 1994]. Efforts to unravel the processes that lead to the formation of life are not new, with attempts to simulate Earth's primitive atmosphere originating over 40 years ago [*Miller*, 1953]. Numerous experiments have been carried out to simulate the synthesis of organic molecules in Titan's atmosphere, including UV radiation, high-energy particles (H^+, e, γ), and electric discharges. These laboratory simulations of Titan's atmosphere produce a remarkable mixture of C_2 through C_6 compounds as well as various nitriles [*Cabane and Chassefière*, 1995].

Hydrogen cyanide (HCN), cyanoacetylene (HC_3N), and cyanogen (C_2N_2) have been identified as components of Titan's atmosphere with the Voyager 1 infrared spectrometer (IRIS) [*Coustenis*, 1990; *Coustenis et al.*, 1991], while ethanenitrile (CH_3CN), commonly referred to as acetonitrile, methyl cyanide, or cyanomethane, has been detected via ground-based millimeter spectroscopy [*Bézard et al.*, 1993]. The models of *Lara et al.* [1996], *Toublanc et al.* [1995], and *Yung et al.* [1987] and *Yung* [1984] postulate that HCN is formed from the reaction of ground state nitrogen atoms when they react with ground state methylene:

(R1) $N(^4S) + {}^3CH_2 \rightarrow HCN + H$

Yung et al. also included the reaction of ground state nitrogen with methyl radicals.

(R2) $N(^4S) + CH_3 \rightarrow HCN + H_2$

Toublanc et al. [1995] and *Lara et al.* [1996] proposed the following mechanism for the formation of CH_3CN:

$$HCN + h\nu \rightarrow CN + H$$

$$CN + CH_4 \rightarrow CH_3CN + H$$

(R3) net: $HCN + CH_4 \rightarrow CH_3CN + H$

Lara et al. also included a second photochemical process involving ethane:

$$HCN + h\nu \rightarrow CN + H$$

$$CN + C_2H_6 \rightarrow CH_3CN + CH_3$$

(R4) net: $HCN + C_2H_6 \rightarrow CH_3CN + CH_3$

Paper number 97JE02526.
0148-0227/97/97JE-02526$09.00

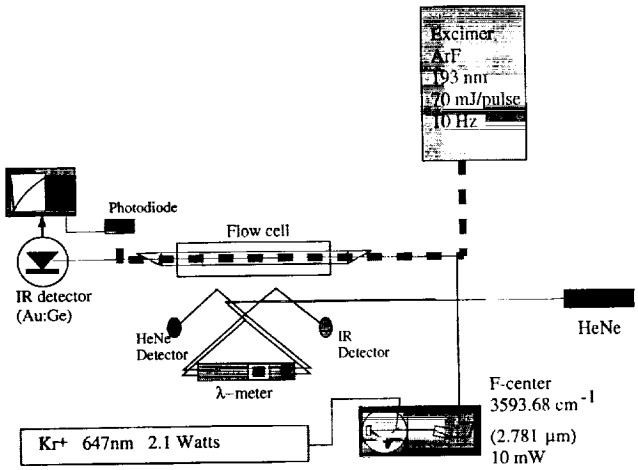

Figure 1. Schematic of experimental setup.

The main loss processes for CH_3CN are considered to be photolysis and vapor condensation.

These compounds, as well as acetylene and the corresponding radicals, are the main chemical species thought to be involved in the production of complex nitriles. Each of the above models for Titan include the following two schemes for the production of cyanoacetylene, HC_3N:

$$C_2H_2 + h\nu \rightarrow C_2H + H$$

$$C_2H + HCN \rightarrow HC_3N + H$$

(R5) net: $C_2H_2 + HCN \rightarrow HC_3N + 2H$

$$HCN + h\nu \rightarrow H + CN$$

$$CN + C_2H_2 \rightarrow HC_3N + H$$

(R6) net: $C_2H_2 + HCN \rightarrow HC_3N + 2H$

The competing, exothermic H atom abstraction reaction, $C_2H + HCN \rightarrow C_2H_2 + CN$, was not considered.

The current research is focused on the reactivity of the ethynyl radical, C_2H, with HCN and CH_3CN:

(R7a) $C_2H + HCN \rightarrow$ products

(R8a) $C_2H + CH_3CN \rightarrow$ products

There are no experimental data to define the products of these reactions. Both hydrogen abstraction reactions and addition/elimination processes are thermodynamically possible:

(R7b) $C_2H + HCN \rightarrow C_2H_2 + CN$

$\Delta H_{rxn} = -38$ kJ mol^{-1}

(R7c) $C_2H + HCN \rightarrow HC{\equiv}CC{\equiv}N + H$

$\Delta H_{rxn} = -126$ kJ mol^{-1}

(R8b) $C_2H + CH_3CN \rightarrow C_2H_2 + CH_2CN$

$\Delta H_{rxn} = -180$ kJ mol^{-1}

(R8c) $C_2H + CH_3CN \rightarrow HC{\equiv}CC{\equiv}N + CH_3$

$\Delta H_{rxn} = -150$ kJ mol^{-1}

(Values of ΔH_{rxn} are calculated on the basis of available ΔH_f^0 values from *Weast* [1990] except for cyanoacetylene, which is from *Okabe and Dibeler* [1973].)

The measurements presented here for the reaction rates of C_2H with the nitrogen containing species, HCN and CH_3CN, are the first direct measurements of the total rate coefficients for these reactions. Since acetylene and polyynes are some of the primary photochemically active species in the atmosphere of Titan, the coupling of the resulting C_2H radicals with the potentially reactive nitrogen compounds is important. In this paper, rate constants for the reactions of C_2H with HCN and CH_3CN are obtained; possible product pathways and the impact of the results on photochemical models are discussed.

2. Experiment

The experimental technique used in the determination of low-temperature rate coefficients of the ethynyl radical has been described in detail [*Pedersen et al.*, 1993; *Opansky and Leone*, 1996], and only a brief overview is presented here. A schematic of the experimental arrangement is shown in Figure 1. The ethynyl radicals are produced by photolysis of acetylene in a flow cell using a pulsed excimer laser operating at 193 nm (70 mJ/pulse at 10 Hz). The transient decay of the C_2H concentration is probed by a single-mode infrared F-center laser operating at 3593.68 cm^{-1}, which is used to monitor the absorption of the $Q_{11}(9)$ line of the $A^2\Pi - X^2\Sigma^+$ (000) transition. The longitudinal mode structure of the F-center laser is monitored with a scanning Fabry-Perot spectrum analyzer, and a traveling wave meter is used for measuring the wavelength [*Hall and Lee*, 1976].

The kinetic experiments are performed in a 1 m long, 2.5 cm diameter, variable temperature flow cell. The photolysis and probe lasers are overlapped over the full length of the cell, and a three-times multipass of the probe beam is employed to increase the absorption path length. Gases are introduced into and removed from the cell via a series of transverse inlets and pump-outs, which allows rapid removal of the photolysis products from the probe volume. The cell was cooled by the circulation of pentane or isobutane through an outer jacket after having passed through a copper coil submerged in an ethanol/liquid nitrogen slush bath. Temperatures of ≈155 K are easily obtained with this method. Due to the slowness of the C_2H + HCN reaction and the limited vapor pressure of CH_3CN, measurements were restricted to low temperatures of 297 K for HCN and 262 K for CH_3CN. Measurements above room temperature to ≈360 K are made by circulating water through the outer jacket while the copper coils are placed in a water reservoir in which the temperature is controlled by an immersion heater. The temperature in the flow cell is measured by three K-type thermocouples positioned along the length of the cell, and partial pressures of each gas are calculated from the measured flow rates using calibrated mass flow meters and the total pressure. Typical number densities for C_2H_2 are (2–6) × 10^{14} cm^{-3}; number densities for HCN and CH_3CN are (0.5–3) × 10^{16} cm^{-3} and (2–8) × 10^{16}, respectively, with a buffer gas of helium in large excess. Using an absorption cross section for C_2H_2 at 193 nm of 1.35 × 10^{-19} cm^{-2} and a quantum yield of 0.26 [*Satyapal and Bersohn*, 1991], the upper limit for $[C_2H]$ is estimated to be 6.5 × 10^{11} cm^{-3}. The total pressure for typical data acquisition on the CH_3CN reaction is between 3.7 and 4.1 kPa (28–31 torr); pressure dependence measurements are conducted over the range of 1.3–12 kPa (10–90 torr). Reaction

rates were independent over this pressure range. The total pressure for data acquisition on the HCN reaction is between 3.7 and 12 kPa (28–90 torr), and the reaction was assumed to be independent of pressure over this range. This large pressure range was required because of the use of a 1% HCN mixture in He; therefore the number density of He is directly related to the possible HCN concentrations obtained. All gases flow through a mixing cell before entering the low-temperature cell. He, 99.99%, C_2H_2, 99.6%, and HCN, 1.0% in helium, are obtained from commercial sources, and most gases are used as received, except acetylene, from which acetone was removed by an activated charcoal filter. Commercially available liquid CH_3CN, 99.9%, was vacuum distilled and degassed.

The probe beam is directed onto a 50 MHz liquid N_2 cooled Ge:Au infrared detector with a sensitive area of 20 mm^2. The transient signals are amplified and co-added using a digital oscilloscope to improve the signal-to-noise ratio. About 1500–3000 transient absorption signals are averaged before the data are transferred to a personal computer, where the data are stored and analyzed.

3. Results

Rate coefficients are measured under pseudo-first-order conditions where [HCN], [CH_3CN], and [C_2H_2] are $\gg$ [C_2H]. The rate of change for [C_2H] can be expressed as

$$d[C_2H]/dt = -[C_2H](k_{RCN}[RCN] + k_{acetylene}[C_2H_2]) \quad (1)$$

where R represents either H or CH_3. After integration of (1),

$$[C_2H] = [C_2H]_0 \exp[-k_{obs}(t)] \quad (2)$$

where

$$k_{obs} = k_{RCN}[RCN] + k_{acetylene}[C_2H_2] \quad (3)$$

$$k_{obs} - k_{acetylene}[C_2H_2] = k_{RCN}[RCN] = k'_{RCN} \quad (4)$$

The observed decay rates of C_2H, k_{obs}, are obtained by fitting the transient signal to the following equation:

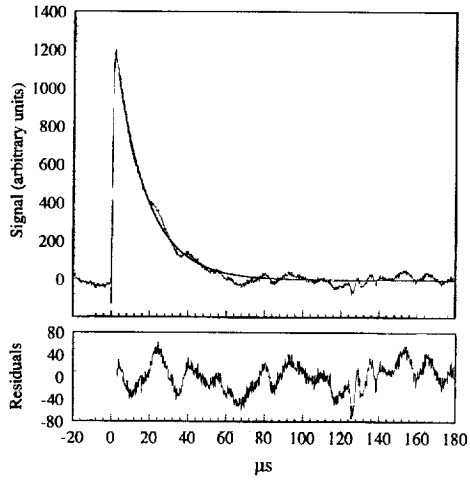

Figure 2. (upper trace) Typical C_2H transient absorption signal at T = 360 K, total pressure 12.3 kPa, [C_2H_2] = 2.8×10^{14} molecules cm^{-3}, [HCN] = 2.5×10^{16} molecules cm^{-3}, and k_{obs} = 0.059 ± 0.001 μs^{-1} (uncertainty represents 95% confidence limit). (lower trace) Residuals to fitted experimental decay.

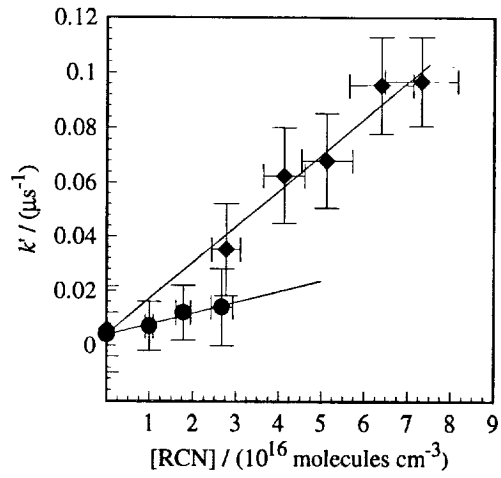

Figure 3. Plot of k'_{RCN} versus [RCN]: diamonds, CH_3CN at T = 296 K and k_{CH_3CN} = (1.3 ± 0.2) × 10^{-12} cm^3 molecules $^{-1}$ s^{-1}; circles, HCN at T = 297 K and k_{HCN} = (3.9 ± 1.2) × 10^{-13} cm^3 $molecules^{-1}$ s^{-1}.

$$y = A \exp[-k_{obs}(t)] + \text{const} \quad (5)$$

An example of a typical C_2H experimental decay and corresponding fit for the reaction with HCN is shown in Figure 2. The values of k_{obs} are corrected for the C_2H + C_2H_2 contribution by subtraction in (4) using the most recent measurements for $k_{acetylene}$ [*Opansky and Leone*, 1996]. The contribution of $k_{acetylene}$ to k_{obs} is between 35 and 70% for the determination of k_{HCN} and less than 40% for the determination of k_{CH_3CN}. The resulting k'_{RCN} values are plotted as a function of concentration and fit using a linear least squares routine. The resultant slope is equal to k_{RCN}; this is shown in Figure 3 for HCN and CH_3CN. The uncertainty in k_{RCN} is determined by computing the standard deviation of the mean for each of the plots of k_{RCN}. The reported errors are $\pm 2\sigma$. The experimental results for C_2H + HCN and CH_3CN are summarized in Table 1, and the corresponding Arrhenius plots are shown in Figure 4. The data can be expressed using the Arrhenius forms $k_{RCN} = A \exp[(E_a)/(RT)]$ as k_{HCN} = (5.3 ± 2.2) × 10^{-12} exp [(−6.4 ± 1.2 kJ/mol)/(RT)] and k_{CH_3CN} = (1.8 ± 1.2) × 10^{-11} exp [(−6.4 ± 2.0 kJ/mol)/(RT)]. The relatively large uncertainty of the Arrhenius parameters is due to the narrow temperature range of the experiments. The observed transient signals can be fit to first-order exponential decays. The standard deviation of each rate constant at a given temperature is taken as the overall experimental uncertainty of each data point (20–30%). The most likely source of systematic error is a reduction in the actual number density of the reactant species due to condensation. The ex-

Table 1. Summary of Rate Constants for C_2H + RCN

Temperatures, K	k_{HCN}	Temperature, K	k_{CH_3CN}
297	(3.9 ± 1.2) × 10^{-13}	262	(1.0 ± 0.2) × 10^{-12}
330	(4.9 ± 1.3) × 10^{-13}	296	(1.3 ± 0.2) × 10^{-12}
360	(6.2 ± 1.8) × 10^{-13}	296	(1.2 ± 0.2) × 10^{-12}
		360	(2.2 ± 0.3) × 10^{-12}

Here k_{HCN} = (5.3 ± 2.2) × 10^{-12} exp [(−6.4 ± 1.2 kJ/mol)/(RT)]; k_{CH_3CN} = (1.8 ± 1.2) × 10^{-11} exp [(−6.4 ± 2.0 kJ/mol)/(RT)]. Values are in units of cm^3 $molecules^{-1}$ s^{-1}.

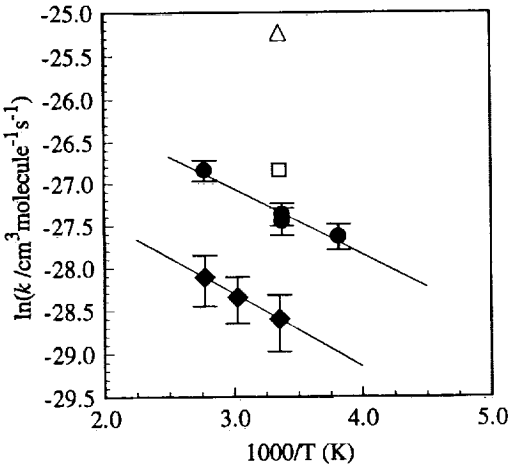

Figure 4. Arrhenius plot: Diamonds, C_2H + HCN; solid line, $k_{HCN} = 5.3 \times 10^{-12}$ exp [(−6.4 kJ/mol)/(R*T*)] cm^3 molecules^{-1} s^{-1}; circles, C_2H + CH_3CN; solid line, $k_{CH_3CN} = 1.8 \times 10^{-11}$ exp [(−6.4 kJ/mol)/(R*T*)] cm^3 molecules^{-1} s^{-1}; open squares, rate constant for the reaction C_2H + HCN → HC_3N + H used in the photochemical models of *Yung et al.* [1984], *Yung* [1987], and *Toublanc et al.* [1995]; and open triangle shows rate constant for the reaction C_2H + HCN → HC_3N + H used in the photochemical model of *Lara et al.* [1996].

periments involving HCN were all performed at temperatures ≥297 K, where HCN does not condense; however, in the case of CH_3CN, attempts to measure rate constants below 262 K resulted in erratic pressure measurements, attributed to condensation of CH_3CN in the flow cell.

Under the current experimental conditions, the minimum C_2H_2 density necessary for detection of the C_2H radical is approximately 1×10^{11} molecules cm^{-3}. The rate constant for the reaction of C_2H with the precursor C_2H_2 is rapid, 1.36×10^{-10} cm^3 molecule^{-1} s^{-1} at 298 K [*Pederson et al.*, 1993; *Opansky and Leone*, 1996]. The combination of this extremely fast reaction and the high density of HCN needed to make rate coefficient measurements presents a serious limitation in the current experiment. Thus we are able to measure the HCN reaction only at temperatures of 297 K and above. An attempt to measure the rate constant at 200 K was made to determine whether the rate might show non-Arrhenius behavior and increase again at even lower temperatures; however, there was no evidence that the rate increases at this temperature, and only the experimental decay from the reaction of C_2H with the precursor molecule acetylene was observable. Use of a pure sample of HCN would allow for higher densities of the reactant and thus increase the observed first-order decay rate; however, this would also lead to larger concentrations of CN radicals from the resulting HCN photolysis (under the current experimental conditions, the CN radical concentration is estimated to be of the same order as C_2H). Another solution would be to improve the sensitivity of the experimental arrangement, by implementing a two-detector signal subtraction scheme to reduce noise from amplitude fluctuations in the laser. Nevertheless, limitations due to the HCN vapor pressure would also make lower temperature measurements difficult. This vapor pressure limitation is observed for CH_3CN. Although the lowest possible experimental temperature is approximately 150 K, rate constants for CH_3CN could only be determined above 262 K. Measurements at temperatures below 262 K were not possible because of condensation of the CH_3CN vapor.

4. Discussion

The experimental results for the reactions of C_2H + HCN and C_2H + CH_3CN show positive temperature dependencies, indicating barriers to reaction, as well as small rate coefficients.

There has been one previous study that examined only the overall product photochemistry of acetylene and hydrogen cyanide mixtures [*Becker and Hong*, 1983]. In those experiments, photolysis of C_2H_2 and HCN mixtures were exposed to 185 nm light from a low-pressure mercury lamp (10^7 photons/s) for 2 min. Gaseous products were then analyzed by gas chromatography/mass spectroscopy. Photolysis products for 5:1 mixtures of HCN/C_2H_2 were similar to those of C_2H_2 (where C_4H_2, diacetylene, was the major product) except for the formation of a significant amount of acrylonitrile, C_2H_3CN. Trace amounts of HC_3N were reported. Under these conditions, only 10% of the light is absorbed by HCN. At higher HCN/C_2H_2 ratios, where 40–60% of the light is absorbed by HCN, HC_3N becomes a major product. As discussed above, the formation of HC_3N is believed to be generated by the possible reactions

$$\text{(R7c')} \qquad C_2H + HCN \rightarrow HC_3N + H \qquad \Delta H_{rxn} = -126 \text{ kJ mol}^{-1}$$

$$\text{(R9)} \qquad CN + C_2H_2 \rightarrow HC_3N + H \qquad \Delta H_{rxn} = -88 \text{ kJ mol}^{-1}$$

Becker and Hong concluded that reaction (R9) was the major process for the formation of HC_3N in their photochemical studies, even though both reactions are exothermic.

The temperature dependence of the kinetic rate coefficients can provide information on the possible mechanisms of the chemical reactions. Although data have been obtained at only three temperatures, the rate constant for C_2H + HCN is decreasing substantially with decreasing temperature. Attempts to measure rate constants at temperatures below 297 K were not possible because of the slow rate of the reaction. A positive temperature dependence and large activation energy are typical of either hydrogen abstraction reactions or addition/elimination reactions that proceed over a barrier in the reaction coordinate. An Arrhenius plot that has little or no temperature dependence or a negative temperature dependence is often associated with an addition/elimination reaction.

In order to better understand the possible pathways for the reaction C_2H + HCN → products, ab initio calculations have been carried out on the transition states corresponding to both the addition/elimination process (products = HC_3N + H) and the hydrogen abstraction mechanism (products = C_2H_2 + CN). The calculations are carried out with a commercial software package using the 6-31 g (d,p) basis set [*Frisch et al.*, 1995]. Geometries for both transition states and individual molecules are calculated using full Møller-Plesset second-order perturbation theory (MP2). Transition state structures are confirmed in a corresponding vibrational frequency calculation [*Foresman and Frisch*, 1996]. Final energies are calculated using the quadratic configuration interaction with single and double excitation substitutions (QCISD). The results of these calculations are shown in Figure 5. Classic barriers are determined without corrections for zero-point or thermal energies. The results show that the transition state corresponding

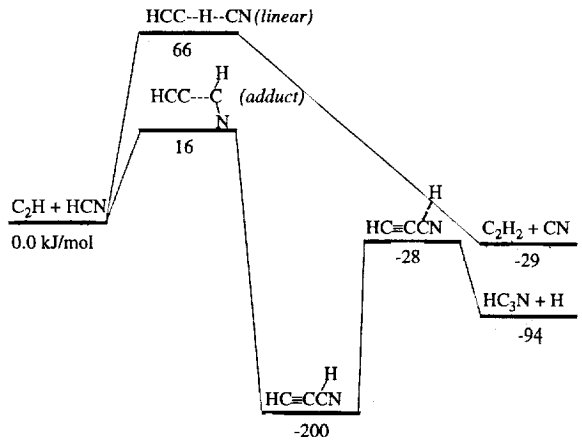

Figure 5. Energy diagram showing classic barrier heights for the reaction C_2H + HCN → products. Calculations carried out using QCISD/6-31g(d,p)//MP2(full)/6-31g(d,p) method.

to the hydrogen abstraction mechanisms lies approximately 43 kJ mol^{-1} (10 kcal mol^{-1}) higher in energy than the transition state for the addition/elimination mechanism, which suggests that the addition/elimination mechanism is the dominant reaction pathway. Although the calculated classic barrier of 15.9 kJ mol^{-1} (3.8 kcal mol^{-1}) overestimates the experimental value of 6.4 kJ mol^{-1} (1.5 kcal mol^{-1}), the presence of a barrier along the reaction coordinate agrees qualitatively with the observed positive temperature dependence.

The measurements for the reaction of C_2H with CH_3CN give rate constants that are very close to those measured previously for methane, CH_4 ($k_{methane} = 1.2 \times 10^{-11}$ exp [(−4.1 kJ/mol)/(RT)]: $154 < T < 359$). Over the observed temperature range, the reaction has a positive temperature dependence and large activation energy. The slower reaction rate for CH_3CN (compared to CH_4) could represent a steric factor due to the presence of the CN group of the CH_3CN; however, based on the experimental measurements and calculations for the C_2H + HCN reaction, an addition/elimination mechanism is likely to contribute to the observed rate constant for C_2H with CH_3CN.

Since this is the first experimental work to directly measure the rate coefficients for reactions (R7a), it is useful to make the comparison with the analogous reactions involving the CN radical, which is isoelectronic with C_2H:

(R10) $CN + HCN \rightarrow C_2N_2 + H$ $\Delta H = -43$ kJ mol^{-1}

Yang et al. [1992] measured rate coefficients for reaction (R10) over the temperature range of 300–740 K. They report room temperature rate constants of $\approx 2.6 \times 10^{-14}$ cm^3 $molecules^{-1}$ s^{-1} and fit their results to the modified Arrhenius equation $k_{R10} = 2.5 \times 10^{-17} T^{1.71}$ exp $(-770/T)$ cm^3 $molecules^{-1}$ s^{-1}. In those experiments, only the disappearance of CN was monitored, and no information was obtained on the product channels. The result corresponds to the present work on C_2H + HCN, in that the rate constant for the addition/elimination reaction is relatively small and the reaction shows a strong positive temperature dependence. *Yang et al.* [1992] calculated a reaction barrier of 13.8 kJ mol^{-1} (3.3 kcal mol^{-1}) for the reaction $CN + HCN \rightarrow H(CN)_2 \rightarrow H + C_2N_2$.

5. Implications for Formation of Cyanoacetylene on Titan

We first focus on the implications of this work for the chemical formation of cyanoacetylene, HC_3N. Photochemical models of Titan have used various rate constants for reactions (R7c), $C_2H + HCN \rightarrow HC_3N + H$ and (R9), $CN + C_2H_2 \rightarrow HC_3N + H$, which are summarized in Table 2. The rate coefficients used in the models for (R7c), also shown in Figure 4, can be compared to the experimental results obtained here. The results show that the rate constant used in the most recent photochemical model [*Lara et al.*, 1996] is too fast by almost a factor of 30 when compared to the room temperature values obtained here. The two earlier models [*Yung et al.*, 1984; *Yung*, 1987; *Toublanc et al.*, 1995] use a value which is only a factor of 5 faster than the measured room temperature results. If we make the assumption that the reaction follows the measured Arrhenius behavior, the expected rate constant would be $\approx 1 \times 10^{-13}$ at 200 K and $\approx 5 \times 10^{-14}$ at 170 K (the latter temperature being close to the value of the lower stratosphere on Titan) and the discrepancy only increases.

The photochemical models of Titan make comparisons of their vertical distributions of cyanoacetylene with available Voyager/IRIS data. *Lara et al.* [1996] pointed out a discrepancy between the mixing ratio of HC_3N determined by Voyager/IRIS data and the value in their model profiles. The results showed that the concentration and column density depended strongly on the eddy diffusion coefficient. Using the eddy diffusion coefficient proposed in their model resulted in vertical profiles for the HC_3N mixing ratio that were too high by nearly 2 orders of magnitude when compared with the available Voyager/IRIS data. Lara et al. noted that the most important reactions in their modeling of HC_3N production are reactions (R7c) and (R9). As mentioned above, the rate constant for (R7c) used in their photochemical model is nearly a factor of 30 faster than the value measured in the current experiments. That value of the rate constant was recommended by *Monks et al.* [1993] assuming analogous behavior with the addition/elimination reaction $C_2H + C_2H_2$ (C_2H_4) → C_4H_2 (C_4H_4) + H. The overprediction of HC_3N may be further aggravated by the rate constant used for reaction (R9). Using the non-Arrhenius expression given by *Lara et al.* [1996], the rate cal-

Table 2. Comparison of Experimental Rate Constants for Reactions Leading to HC_3N With Values Used in Recent Photochemical Models of Titan

Reaction	Experiment	*Yung et al.* [1984]	*Yung* [1987]	*Toublanc et al.* [1995]	*Lara et al.* [1996]
$C_2H + HCN \rightarrow HC_3N + H$	$5.3 \times 10^{-12} e^{(-770/T)}$ [a]	2.2×10^{-12}	···	2.2×10^{-12}	1.1×10^{-11}
$CN + C_2H_2 \rightarrow HC_3N + H$	$\approx 4 \times 10^{-10}$ [b]	5×10^{-11}	2.3×10^{-11}	$3.49 \times 10^{-11} e^{(571/T)}$	$5.67 \times 10^{-9} T^{0.55} e^{(-4/T)}$

Values are in units of cm^3 $molecules^{-1}$ s^{-1}.
[a]Current results.
[b]From *Sims et al.* [1993], $25 < T < 80$ K.

Table 3. Parameters and Production Rates of HC_3N Via C_2H + HCN and CN + C_2H_2 Reaction Pathways

Parameter	*Yung et al.* [1984]	*Toublanc et al.* [1995]	*Lara et al.* [1996]
$[C_2H]$ at 750 km	$\approx 3 \times 10^3$ molecules cm^{-3}		
[CN] at 750 km	$\approx 1 \times 10^2$ molecules cm^{-3}		
Mixing ratio HCN	10^{-4}	10^{-4}	2×10^{-5} at 400 km[a]
Mixing ratio C_2H_2	7×10^{-4}	1.5×10^{-3}	8×10^{-4}
$k(C_2H + HCN)$[b]	2.2×10^{-12}	2.2×10^{-12}	1.1×10^{-11}
$k(CN + C_2H_2)$	5×10^{-11}	1×10^{-11} (T = 170 K)	9×10^{-8} (T = 170 K)
n(750 km)	5×10^{11} molecules cm^{-3}		

	Production Rates of HC_3N, molecules cm^{-3} s^{-1}			
Reaction Pathway	This work	*Yung et al.* [1984]	*Toublanc et al.* [1995]	*Lara et al.* [1996]
$C_2H + HCN \rightarrow HC_3N + H$	0.008[c]	0.3	0.5	0.3
$CN + C_2H_2 \rightarrow HC_3N + H$	14[d]	2	75	3600

[a]Assumed to have small variance between 400 and 750 km.
[b]All rate constants have units cm^3 $molecules^{-1}$ s^{-1}.
[c]Using $k = 5 \times 10^{-14}$ (from Arrhenius expression at 170 K based on this work).
[d]Using $k = 4 \times 10^{-10}$ [from *Sims et al.*, 1993].

culated at 170 K would be 9.3×10^{-8} cm^3 $molecules^{-1}$ s^{-1}. This rate is nearly 2 orders-of-magnitude faster than the gas-kinetic rate. In addition, *Sims et al.* [1993] recently reported the rate coefficient for reaction (R9) down to 25 K. At temperatures below 100 K the rate constant is $\approx 4 \times 10^{-10}$ cm^3 $molecules^{-1}$ s^{-1}, very close to the gas-kinetic rate. Between 100 and 200 K the reaction rate is still very fast, 2–3 $\times$ 10^{-10} cm^3 $molecules^{-1}$ s^{-1}. The large difference in the rate used in the model may be responsible for the source of discrepancy in the computed vertical distributions of HC_3N.

The models of *Yung et al.* [1984; *Yung*, 1987] and *Toublanc et al.* [1995] used the same, estimated value for the rate constant of reaction (R7c), $C_2H + HCN \rightarrow HC_3N + H$; however, their use of significantly different values of the rate constant for reaction (R9), $CN + C_2H_2 \rightarrow HC_3N + H$, make direct comparison between the models difficult. Other factors in addition to the difference in rate constants (e.g., the eddy diffusion coefficient, reactivity of HC_3N, photolysis rate) contribute to the observed differences in the vertical profiles of HC_3N. *Coustenis* [1990] sets an upper limit for the equatorial mixing ratio for HC_3N at 105 km of $\leq 1.5 \times 10^{-9}$. At the time of the *Yung et al.* [1984] models, only crude estimates were available for the concentration of this species, and their column-averaged abundances for HC_3N were in good agreement with the available data [*Kunde et al.*, 1981]. Examination of the *Yung et al.* [1984] HC_3N vertical profile indicates that the mixing ratio is approximately 10^{-7} at 100 km. However, *Toublanc et al.* [1995] indicate that their mixing ratio of HC_3N at 105 km is $\leq 10^{-12}$, although the stratospheric abundances (450–850 km) of *Toublanc et al.* [1995] appear to be within a factor of 10 of those of *Yung et al.* [1984]. The nitrile photochemistry of *Yung et al.* [1984] was revised [*Yung*, 1987] mainly to include the updated rate constant of the reaction $CN + HCN \rightarrow C_2N_2 + H$ and new chemical schemes for the formation of cyanogen, C_2N_2. However, the overall vertical distributions for the nitrile compounds included in the model changed little from the original work due the inclusion of additional pathways for the formation of C_2N_2.

An evaluation can be carried out to quantify the results presented here in terms of the production rate of HC_3N. The reaction rates for C_2H + HCN and CN + C_2H_2 were calculated for concentrations of molecular species at 750 km. (This altitude was chosen because the mixing ratio of C_2H was at a maximum in the *Yung et al.* [1984] paper.) Concentrations for the radical species C_2H and CN are from *Yung et al.* [1984]. This is the only reference that reports the vertical profiles of these radical species. Concentrations of the molecular species are determined by multiplying the reported mixing ratios (mole fractions) by the total number density at 750 km [*Yung et al.*, 1984]. The data required for this comparison as well as the production rates are shown in Table 3. The models assume that each reaction has only one product channel. This allows one to set the reaction rate for each process equal to the production rate of HC_3N for the particular reaction pathway. It is interesting to note the similarities of the three models for the production of HC_3N via the C_2H + HCN pathway; however, a major difference occurs between the model values and the value obtained using the new rate constant of 5×10^{-14} cm^3 $molecules^{-1}$ s^{-1} (170 K) extrapolated from the Arrhenius expression determined in the present study. Similar estimations were made for the CN + C_2H_2 reaction pathway. It is clear that the CN + C_2H_2 reaction dominates in the production of HC_3N.

It is important to note that while the current paper deals with differences in the rate constants obtained experimentally and those used in photochemical models, other factors also influence the calculated vertical distributions of HC_3N. Processes such as diffusion, mixing as well as loss processes associated with condensation, and chemical reactivity are also important in predicting the concentration of minor atmospheric constituents; however, the use of accurate reaction rates is essential if a complete understanding of the photochemical processes is to be achieved.

Finally, current photochemical models include CH_3CN but limit the loss processes to photolysis and condensation. Since the concentration of CH_3CN on Titan is low and the rate constant presented here is relatively small, the inclusion of the reactions of C_2H with CH_3CN would most likely have little effect on the predicted vertical profiles; however, the reaction $C_2H + CH_3CN \rightarrow HC_3N + CH_3$ does represent a possible additional pathway for the formation of cyanoacetylene, HC_3N.

The variations between the three models demonstrate the need for further refinement in both experimental and theoret-

ical work. The use of updated rate coefficients such as those presented here and by other research groups, as well as a prudent analysis of the reaction pathways should allow future models to better estimate atmospheric abundances of major and minor constituents on Titan. The upcoming Cassini/Huygens mission will greatly enhance our current knowledge of Titan's atmosphere.

Acknowledgment. We gratefully acknowledge the National Aeronautics and Space Administration for support of this research.

References

Becker, R. S., and J. H. Hong, Photochemistry of acetylene, hydrogen cyanide, and mixtures, *J. Phys. Chem.*, *87*, 163–166, 1983.

Bézard, B., A. Marten, and G. Paubert, Detection of acetonitrile on Titan, *Bull. Am. Astron. Soc.*, *25*, 1100, 1993.

Cabane, M., and E. Chassefière, Laboratory simulations of Titan's atmosphere: Organic gases and aerosols, *Planet. Space Sci.*, *43*, 47–65, 1995.

Coustenis, A., Spatial variations of temperature and composition in Titan's atmosphere: Recent results, *Ann. Geophys.*, *8*, 645–652, 1990.

Coustenis, A., B. Bézard, D. Gautier, A. Marten, and R. Samuelson, Titan's atmosphere from Voyager infrared observations, III, Vertical distributions of hydrocarbons and nitriles near Titan's north pole, *Icarus*, *89*, 152–167, 1991.

Foresman, J. B., and A. Frisch, *Exploring Chemistry With Electronic Structure Methods*, 2nd ed., Gaussian, Pittsburgh, Pa., 1996.

Frisch, M. J., et al., Gaussian 94, Revision D.4, Gaussian, Pittsburgh, Pa., 1995.

Gladstone, G. R., M. Allen, and Y. L. Yung, Hydrocarbon photochemistry in the upper atmosphere of Jupiter, *Icarus*, *119*, 1–52, 1996.

Hall, J. L., and S. A. Lee, Interferometric real-time display of cw dye laser wavelength with sub-Doppler accuracy, *Appl. Phys. Lett.*, *29*, 367–369, 1976.

Kunde, V. G., A. C. Aikin, R. A. Hanel, D. E. Jennings, W. C. Maguire, and R. E. Samuelson, C_4H_2, HC_3N, and C_2N_2 in Titan's atmosphere, *Nature*, *292*, 686–688, 1981.

Lara, L. M., E. Lellouch, J. J. López-Moreno, and R. Rodrigo, Vertical distribution of Titan's atmospheric neutral constituents, *J. Geophys. Res.*, *101*, 23,261–23,283, 1996.

Miller, S. L., A production of amino acids under possible primitive Earth conditions, *Science*, *117*, 528–529, 1953.

Monks, P. S., P. N. Romani, F. L. Nesbitt, M. Scanlon, and L. J. Stief, The kinetics of the formation of nitrile compounds in the atmospheres of Titan and Neptune, *J. Geophys. Res.*, *98*, 17,115–17,122, 1993.

Mordaunt, D. H., I. R. Lamber, G. P. Morley, M. N. R. Ashfold, R. N. Dixon, C. M. Western, L. Schneider, and K. H. Welge, Primary product channels in the photodissociation of methane at 121.6 nm, *J. Chem. Phys.*, *98*, 2054–2065, 1993.

Okabe, H., and V. H. Dibeler, Photon impact studies of C_2HCN and CH_3CN in the vacuum ultraviolet: Heats of formation of C_2H and CH_3CN, *J. Chem. Phys.*, *59*, 2430–2435, 1973.

Opansky, B. J., and S. R. Leone, Low temperature rate coefficients of C_2H with CH_4, CD_4 from 150 to 359 K, *J. Phys. Chem.*, *100*, 4888, 1996.

Pedersen, J. O. P., B. J. Opansky, and S. R. Leone, Laboratory studies of low-temperature reactions of C_2H with C_2H_2 and implications for atmospheric models of Titan, *J. Phys. Chem.*, *97*, 6822–6829, 1993.

Raulin, F., P. Bruston, P. Coll, D. Coscia, M.-C. Gazeau, L. Guez, and E. De Vanssay, Exobiology on Titan, *J. Biol. Phys.*, *20*, 39–53, 1994.

Satyapal, S., and R. Bersohn, Photodissociation of acetylene at 193.3 nm, *J. Phys. Chem.*, *95*, 8004–8006, 1991.

Sims, I. R., J. L. Queffelec, D. Travers, B. R. Rowe, L. B. Herbert, J. Karthäuser, and I. W. M. Smith, Rate constants for the reactions of CN with hydrocarbons at low and ultra-low temperatures, *Chem. Phys. Lett.*, *211*, 461–468, 1993.

Toublanc, D., J. P. Parisot, J. Brillet, D. Gautier, F. Raulin, and C. P. McKay, Photochemical modeling of Titan's atmosphere, *Icarus*, *113*, 2–26, 1995.

Weast, R. C. (Ed.), *CRC Handbook of Chemistry and Physics*, CRC, Boca Raton, Fla., 1990.

Yang, D. L., M. C. Lin, and C. F. Melius, CN radical reactions with hydrogen cyanide and cyanogen: Comparison of theory and experiment, *J. Chem. Phys.*, *97*, 222–226, 1992.

Yung, Y. L., An update of nitrile photochemistry on Titan, *Icarus*, *72*, 468–472, 1987.

Yung, Y. L., M. Allen, and J. P. Pinto, Photochemistry of the atmosphere of Titan: Comparison between model and observations, *Astrophys. J. Suppl.*, *55*, 465–506, 1984.

R. J. Hoobler and S. R. Leone, JILA, University of Colorado at Boulder, Campus Box 440, Boulder, CO 80309-0440. (e-mail: srl@jila.colorado.edu)

(Received June 11, 1997; revised September 3, 1997; accepted September 9, 1997.)